Bull Earthquake Eng (2010) 8:1267–1294
DOI 10.1007/s10518-010-9181-y

ORIGINAL RESEARCH PAPER

Displacement capacity of masonry buildings as a basis for the assessment of behavior factor: an experimental study

Miha Tomaževič · Polona Weiss

Received: 16 July 2009 / Accepted: 19 March 2010 / Published online: 2 April 2010

Abstract The results of shaking table tests of a series of 1:5 scale masonry building models have been used for the assessment of values of structural behavior factor q for masonry structures, seismic force reduction factors proposed for the calculation of design seismic loads by Eurocode 8, European standard for the design of structures for earthquake resistance. Six models have been tested, representing prototype buildings of two different structural configurations and built with two different types of masonry materials. The study indicated that the reduction of seismic forces for the design depends not only on the type of masonry construction system, but also on structural configuration and mechanical characteristics of masonry materials. It has been also shown that besides displacement and energy dissipation capacity, damage limitation requirement should be taken into account when evaluating the values of behavior factor. On the basis of analysis of experimental results a conclusion can be made, that the values at the upper limit of the proposed range of values of structural behavior factor q for unreinforced and confined masonry construction systems are adequate, if push-over methods are used and the calculated global ductility of the structure is compared with the displacement demand. In the case where elastic analysis methods are used and significant overstrength is expected, the proposed values are conservative. However, additional research and parametric studies are needed to propose the modifications.

Keywords Masonry · Shaking-table tests · Models · Displacement capacity · Damage limitation · Design seismic load · Earthquake resistance · Behavior factor

1 Introduction

According to European standard for earthquake resistant design of structures, Eurocode 8 (2004), the structure should be designed to withstand the earthquake with return period 475 years and 10% probability of exceedance in 50 years, "without local or global collapse,

M. Tomaževič (✉) · P. Weiss
Slovenian National Building and Civil Engineering Institute, Dimičeva 12, 1000 Ljubljana, Slovenia
e-mail: miha.tomazevic@zag.si

thus retaining its structural integrity and a residual load bearing capacity after the seismic events" (no collapse requirement). However, the structure shall be also designed to withstand an earthquake having a larger probability of occurrence than the design earthquake, i.e. earthquake with return period 95 years with 10% probability of exceedance in 10 years, "without the occurrence of damage and limitation of use, the costs of which would be disproportionately high in comparison with the costs of the structure itself" (damage limitation requirement). When verifying the seismic resistance, it has to be verified that for all structural members as well as for the structure as a whole, the design resistance capacity R_d, calculated by taking into account the characteristic strength values and partial safety factors γ_M of members' materials, is greater than the design value of combined action effect E_d, which includes seismic actions.

The form of seismic action to be used in seismic resistance verification depends on the importance and complexity of the structure under consideration. In the case of structures with regular structural configuration, such as masonry structures, the calculations are simplified by taking into account only one horizontal component of the seismic ground motion and analyzing the structure in each orthogonal direction separately. Non-linear dynamic response analysis is replaced by equivalent elastic static analysis, where the design seismic loads are evaluated on the basis of the design response spectra, considering the structure as an equivalent single-degree-of-freedom system. To obtain the design spectra, the ordinates of the elastic response spectra are reduced by a factor, which takes into account the displacement and energy dissipation capacity of the structure under consideration. This factor is generally called "force reduction factor" or, by terminology used in European standard for earthquake resistant design, "structural behavior factor q".

Experimental data, on the basis of which the q-factor values in the standard have been proposed, are scarce. In their previous studies the authors of this paper indicated that the values proposed at the lower limit for plain, confined and reinforced masonry may be considered conservative (Tomaževič and Weiss 1994; Tomaževič and Klemenc 1997). In an analytical study, Moroni et al. (1992) found that the proposed values of force reduction factors for confined masonry systems, obtained on the similar basis as in the Eurocode 8, are reasonable. Recently, cyclic lateral resistance tests of walls have been used to assess the values of structural behavior factor (Da Porto et al. 2009).

Alcocer et al. (2004) gave experimental indication regarding the displacement capacity of confined masonry structures in correlation with damage to masonry walls and usability of buildings. Mexican data are in good agreement with the results, which the authors of this paper obtained by testing different other types of masonry. On the basis of such information, damage limitation criteria have been defined (Tomaževič 2007) which have been taken into consideration in this analysis.

To enhance the existing information regarding the possible ranges of values of structural behavior factor q, the seismic behavior of typical Central European masonry buildings with different structural configurations and qualities of masonry materials has been investigated also at Slovenian National Building and Civil Engineering Institute (ZAG) in Ljubljana, Slovenia. The main results of experimental study are presented and discussed in this paper.

2 Experimental program and description of tests

Six models representing buildings of two different structural configurations and constructed with two different types of masonry materials have been tested on a simple uni-directional seismic simulator. Models type M1 (Fig. 1a) represented a two-story terraced house with

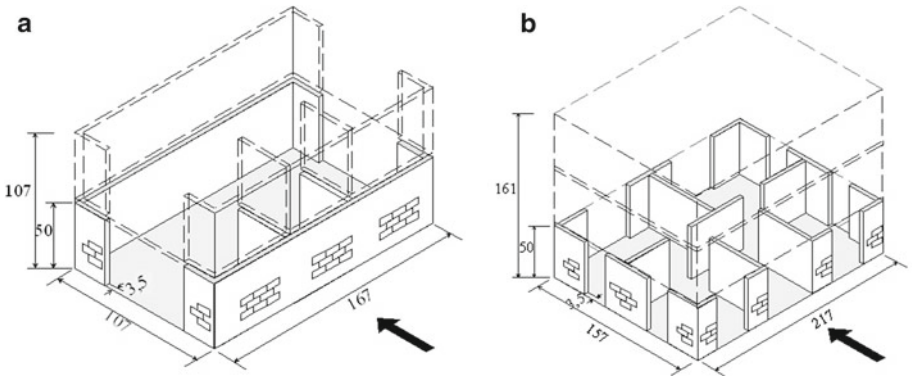

Fig. 1 Configuration and dimensions of models. **a** Terraced house models M1 and **b** apartment house models M2. The arrows indicate the direction of seismic excitation. Dimensions in cm

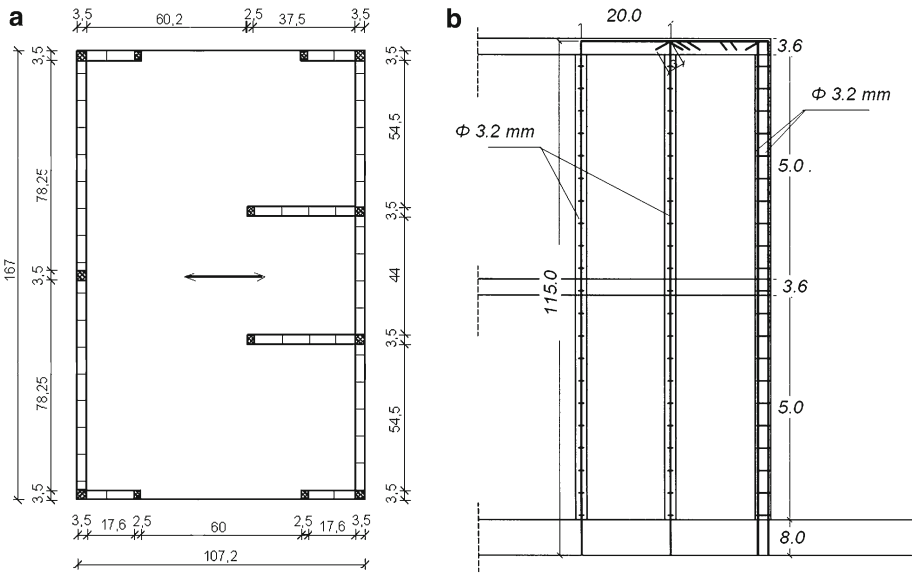

Fig. 2 Disposition of tie-columns of the terraced hose model M1-1-d in plan (**a**) and (**b**) reinforcement of the tie-columns. Dimensions in cm

the main structural walls orthogonal to seismic motion. The length of a typical section of such building is 10 m, and the width is 6 m. Models type M2 (Fig. 1b) represented a three-story apartment house with uniformly distributed structural walls in both directions. Typical dimensions of such prototype building in plan are 18 by 12 m. Four models of the first and two models of the second type have been tested. In the case of the terraced house, two models have been built as either partly (model M1-1c) or completely confined masonry structures (model M1-1d, Fig. 2). The description of the tested models is given in Table 1.

The models have been constructed by respecting the technology of construction and masonry bond of the prototypes. Instead of traditional masonry bond, the internal structural walls of the prototype buildings of both structural configurations are interconnected with peripheral walls by means of steel connectors, placed in each second bed joint at the

Table 1 Description of models

Designation	Type	Masonry	Confinement
M1-1	2-story terraced house	Type 1	No confinement
M1-2	2-story terraced house	Type 2	No confinement
M1-1c	2-story terraced house	Type 1	Confined staircase walls
M1-1d	2-story terraced house	Type 1	Fully confined walls
M2-1	3-story apartment house	Type 1	No confinement
M2-2	3-story apartment house	Type 2	No confinement

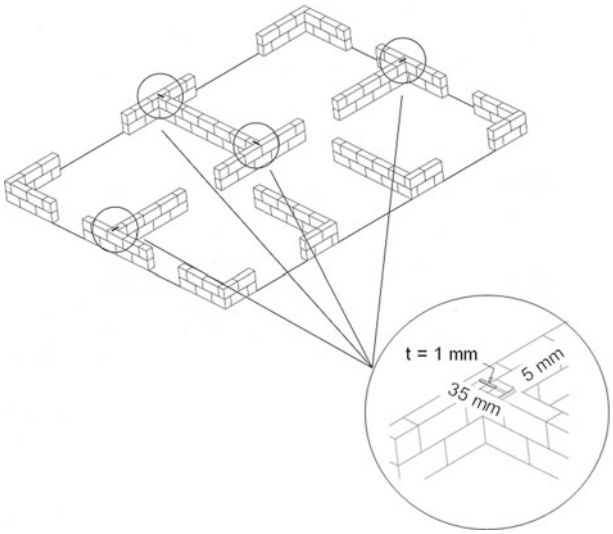

Fig. 3 Masonry bond: internal walls are connected with peripheral walls by means of steel connectors

vertical connection plane between the walls. In the case of the models, steel connectors have been modeled with thin steel strips 35/5/1 mm (length/width/thickness, Fig. 3).

The models, built at 1:5 scale, have been designed by taking into account the laws of complete (true) model similitude (Langhaar 1951; Tomaževič and Velechovsky 1922; Harris and Sabnis 1999). In the case of true models, the strength properties of prototype masonry are reduced at geometrical scale, whereas the strains, specific mass and material damping remain the same as in the case of the prototype. If a quantity q_M is measured on the model, the relationship $q_P = q_M S_q$ applies for the quantity q_P which refers to the prototype, where S_q is a scale factor. The relationships between the model and prototype quantities for the cases of the general and true model similitude are given in Table 2.

When designing the models for the shaking table tests, not all details of structural configuration of the actual buildings have been modeled. As the size of the exact replicas of the actual prototype structures, considered in the design, exceeded the dimensions of the steel platform of the shaking table installed at ZAG, the actual dimensions of the models have been adjusted to fit the platform. Consequently, the dimensions of the prototypes, represented by the tested models are slightly smaller than those of the actual buildings. However, the wall/floor area ratio, slenderness and restraint conditions of the walls remained the same, so that the models

Table 2 Scale factors S_q for main physical quantities: general equations and values for 1:5 scale complete model

Quantity	General equation	Complete model
Length (L)	$S_L = L_P/L_M$	$S_L = 5$
Strain (ε)	$S_\varepsilon = \varepsilon_P/\varepsilon_M$	$S_\varepsilon = 1$
Strength (f)	$S_f = f_P/f_M$	$S_f = S_L = 5$
Stress (σ)	$S_\sigma = f_P/f_M$	$S_\sigma = S_L = 5$
Modulus of elasticity (E)	$S_E = S_\sigma/S_\varepsilon$	$S_E = S_L = 5$
Specific weight (γ)	$S_\gamma = \gamma_P/\gamma_M$	$S_\gamma = 1$
Force (F)	$S_F = S_L^2 S_f$	$S_F = S_L^3 = 125$
Time (t)	$S_t = S_L\sqrt{S_\gamma S_\varepsilon/S_f}$	$S_t = \sqrt{S_L} = 2.24$
Frequency (ω)	$S_\omega = 1/S_L$	$S_\omega = 1/\sqrt{S_L} = 0.45$
Displacement (d)	$S_d = S_L S_\varepsilon$	$S_d = S_L = 5$
Velocity (v)	$S_v = S_\varepsilon\sqrt{S_f/S_\gamma}$	$S_v = \sqrt{S_L} = 2.24$
Acceleration (a)	$S_a = S_f/(S_L S_\gamma)$	$S_a = 1$

adequately represented all structural characteristics of the prototypes. On the basis of the characteristics of structural geometry and model material properties (reduced strength and unchanged specific weight), it can be concluded that both, in-plane and out-of-plane behavior of structural walls have been adequately simulated.

The influence of two different masonry types, typically used in Germany, on the seismic behavior of buildings, has been also studied. To compare the behavior, masonry consisting of calcium silicate units, laid in thin layer, class M15 mortar (masonry Type 1) and masonry consisting of hollow clay units, laid in general purpose, class M5 mortar (masonry Type 2), have been selected (Oetes and Loering 2006). The dimensions of units of both masonry types are 500/250/175 mm (length/height/thickness).

Because of the small scale at which the models have been built and tested, the model units have been manufactured as solid units with gross dimensions and strength scaled according to model similitude rules. For practical reasons, and because the preliminary studies indicated that there is little, if any, influence of the modeled mortar type on the compressive strength of model masonry, only one type of mortar has been used for the construction of model masonry. Model masonry units with dimensions 100/50/35 mm (length/height/thickness) have been made by pouring especially designed mortars, composed of sand, lime, cement, vermiculite and water, into steel form. Several mixes have been tried before the final selection. Model units, representing the calcium silicate blocks have been cast with a mix, consisting of cement, lime and sand in the proportion of 1:1:9. Model units, representing hollow clay blocks, however, have been cast with a mix, consisting of cement, lime, sand and vermiculite in the proportion of 1:1:0.25:6. Portland cement PC 45, hydrated lime and river-bed sand, aggregate size 0–4 mm, have been used.

Lime mortar with a small quantity of Portland cement added in order to accelerate hardening has been used for the construction of both types of models. The mortar consisted of Portland cement PC-45, hydrated lime and river-bed sand (aggregate size 0–1 mm) in the proportion of 0.4:1:11. The added quantity of water was such as to obtain 210 mm diameter flow by the standard flow test.

The mechanical properties of model masonry materials, which control the seismic behavior of model buildings, are correlated with the target prototype values in Table 3. Although several attempts have been made to reduce the mechanical properties of all masonry constituents as close as possible to the requirements of complete modeling, not all physical

Table 3 Correlation between the target prototype and actual model values of mechanical properties of masonry units and masonry

	Quantity	Prototype	Model	$S = P/M$
Type 1:calcium silicate units	Compressive strength of units (MPa)	20.0	6.12	3.3 (5.0)
	Specific weight of units (kN/m^3)	20.0	19.7	1.0 (1.0)
	Compressive strength of masonry (MPa)	15.0	4.54	3.3 (5.0)
	Tensile strength of masonry (MPa)	0.15 – 0.25	0.06	2.5 (5.0)
Type 2:hollow clay units	Compressive strength of units (MPa)	12.0	2.91	4.1 (5.0)
	Specific weight of units (kN/m^3)	7.7	6.8	1.1 (1.0)
	Compressive strength of masonry (MPa)	5.6	1.85	3.0 (5.0)
	Tensile strength of masonry (MPa)	0.14 – 0.19	0.06	2.8 (5.0)

S = the actual scale factor (factors of complete model similitude are given in parentheses)

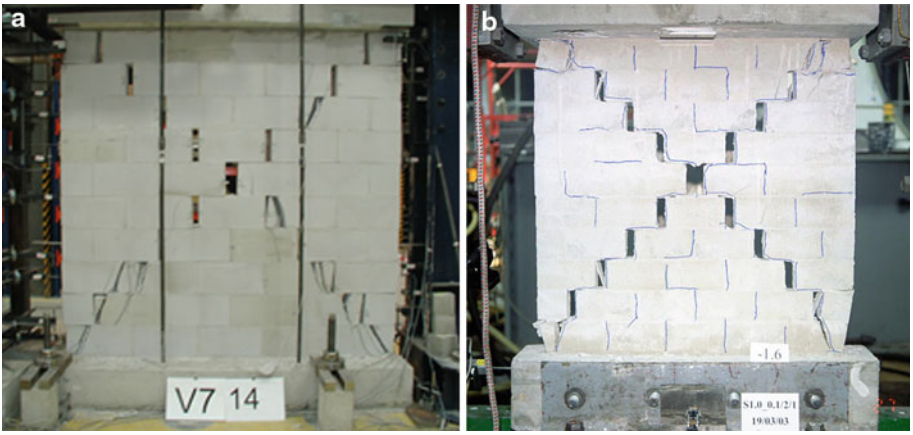

Fig. 4 Typical damage pattern of a prototype (**a**) and (**b**) model calcium silicate units wall at the end of the lateral resistance tests. Fig. 3a adopted from Oetes and Loering (2006)

quantities have been modeled as expected. Despite that, good correlation between the failure mechanisms and damage propagation, resistance and displacement capacity as well as energy dissipation characteristics of the model and prototype masonry walls has been obtained (see Figs. 4 and 5). Failure mechanisms and the shape of hysteretic behavior of the prototype and model masonry walls were almost identical. This indicates that, despite the differences between the target and actually achieved values of mechanical properties of model masonry and masonry constituents, the basic requirements for the similitude in non-linear behavior and failure mechanism have been fulfilled.

By comparing the hysteretic relationships shown in Fig. 5, for example, it can be seen that in terms of displacements, the tested models can be considered as true models. The actual scale factor ($S_d = d_{\max,P}/d_{\max,M} = 16{,}66\,\text{mm}/3{,}11\,\text{mm} = 5{,}36$) is slightly greater than $S_d = S_L = 5$. In terms of resistance, however, the similitude is slightly distorted. The actual scale factor in this case ($S_F = H_{\max,P}/H_{\max,M} = 148{,}49/2{,}02\,\text{kN} = 73{,}5$) would correspond to the modeling scale 1:4,1 instead of 1:5. The distortion should be taken into consideration when referring the results of the model tests to the prototypes.

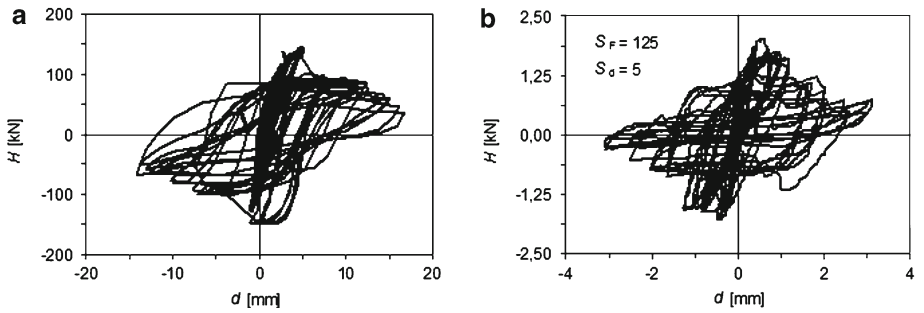

Fig. 5 Hysteresis loops obtained by lateral resistance tests of a prototype (**a**) and (**b**) model calcium silicate units wall. Fig. 5a adopted from Oetes and Loering (2006)

Floor slabs, staircases and vertical confining elements have been made of micro-concrete, with compressive strength reduced according to the rules of complete model similitude and reinforced with steel reinforcement. Since the mechanical properties of steel have not been modeled, the amount of steel has been reduced in accordance with the force modeling factor. Therefore, similar diaphragm action of floors and similar distribution of forces onto the walls has been achieved as in the case of the prototypes. Similarly, micro-concrete and commercially available steel wire with reduced area have been used to reinforce the vertical confining elements of models M1-1c and M1-1d. In the case of model M1-1-d, 4 bars of Φ 3.2 mm fully annealed wire (yield stress 266 MPa) have been placed in the tie-columns at the corners and wall intersections, and 2 Φ 3.2 mm bars in the tie-columns at the ends of the walls. Φ 1.1 mm wire has been used for stirrups (see Fig. 2b).

A gap between the stairs and the floor slabs has been provided at each floor level in order to prevent possible negative effect of the relatively rigid staircase on the seismic response of the models. In order to ensure the similitude of distribution of masses along the height of the tested buildings and similitude of precompression in structural walls (i.e. compressive stress/compressive strength of masonry ratio), the missing live load has been simulated by fixing the adequately distributed steel blocks on the floor slabs. In the case of the terraced house models M1, 170 kg mass was fixed at the first and 290 kg at the second floor level, whereas in the case of the apartment house models M2, 300 kg mass was fixed at the first and the second floor, and 480 kg mass at the third floor level. Additional mass at the top floor included the mass of the roof structure. The masses, concentrated at floor levels, as well as the total mass of the models are given in Table 4, whereas the correlation of wall/floor mass ratio for the prototype and model structures is given in Table 5.

The models have been built on r.c. foundation slabs, bolted to the moveable steel platform of the shaking table. Displacement transducers (LVDTs) and accelerometers have been placed in the center and at both edges of floor slabs at each floor level (Fig. 6). After each test run, the models have been inspected for damage, and the changes in dynamic properties of the models have been determined by analyzing the records of free vibrations obtained by hitting the top slab of the model with impact hammer.

Shaking-table motion simulated the 24 s long strong phase of the north-south component of the ground acceleration record of the Montenegro earthquake of April 15, 1979, obtained at Petrovac, with peak ground acceleration $a_{g,max} = 0.43$ g. The acceleration and displacement time history of the strong phase of the earthquake are shown in Fig. 7, whereas the acceleration response spectra of the record are compared with the Eurocode 8 design spectrum for firm soil in Fig. 8.

Table 4 Masses of masonry walls m_w, floors m_f (dead load) and weights m_l (live load), concentrated at floor levels, and total mass of the models m_{tot} (in kg)

Model		1st floor	2nd floor	3rd floor	Total mass
M1-1	Masonry m_w	178	89	–	
M1-1c	Floor slab m_f	118	118	–	
M1-1d	Weights m_l	170	290	–	
	Total/floor	466	497	–	1052
M1-2	Masonry m_w	61	30	–	
	Floor slab m_f	118	118	–	
	Weights m_l	170	290	–	
	Total/floor	349	428	–	807
M2-1	Masonry m_w	206	206	103	
	Floor slab m_f	218	218	218	
	Weights m_l	300	300	480	
	Total/floor	724	724	801	2352
M2-2	Masonry m_w	70	70	35	
	Floor slab m_f	218	218	218	
	Weights m_l	300	300	480	
	Total/floor	588	588	553	1764

Table 5 Wall/floor mass ratio (m_w/m_{f+l}) of the prototype (P) and model structures (M)

Model	m_{wP} (kg)	$m_{(f+l)P}$ (kg)	$m_{wP}/m_{(f+l)P}$ ratio	m_{wM} (kg)	$m_{(f+l)M}$ (kg)	$m_{wM}/m_{(f+l)M}$ ratio
M1-1	22200	35300	0.63	178	288	0.62
M1-2	10000	35300	0.28	61	288	0.21
M2-1	25700	67900	0.38	206	518	0.40
M2-2	11600	67900	0.17	70	518	0.14

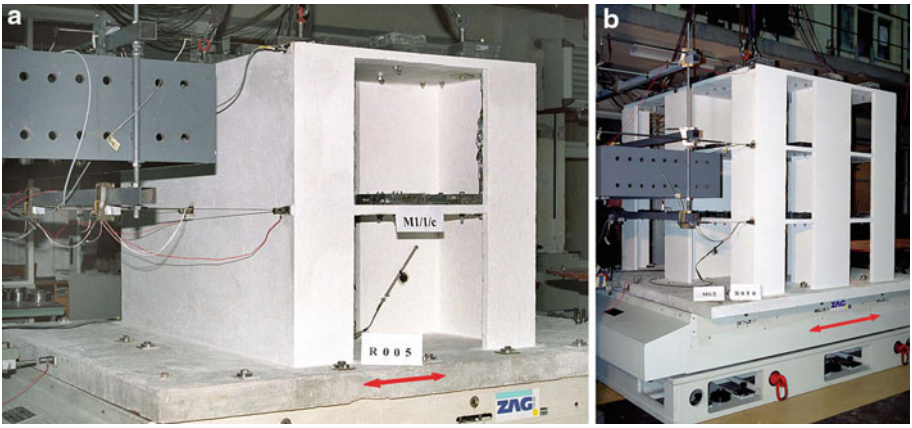

Fig. 6 Instrumentation of models: terraced house model (**a**) and (**b**) apartment house model. *Arrows* indicate the direction of seismic excitation

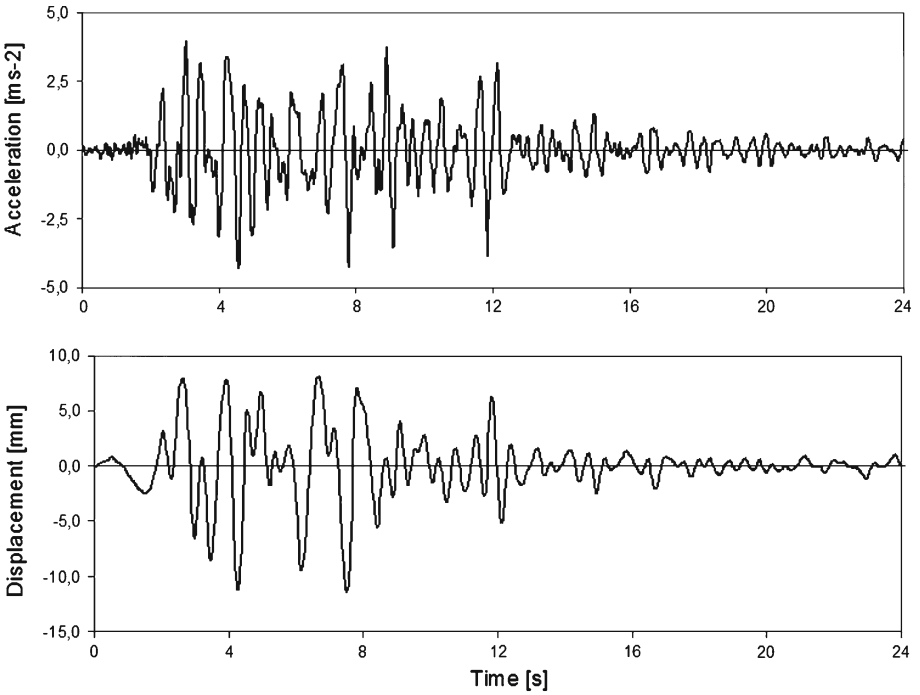

Fig. 7 Acceleration and displacement time history of the N-S component of the 24 s long strong phase of the Montenegro earthquake of April 15, 1979, Petrovac record

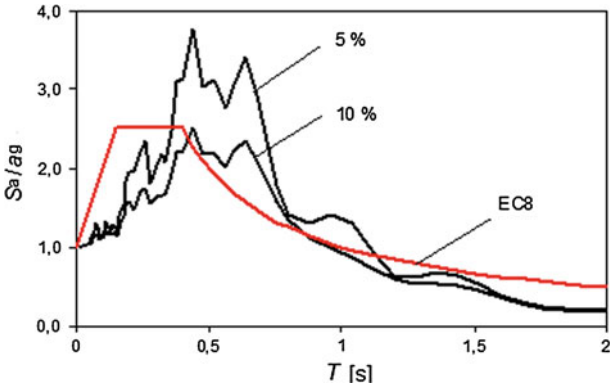

Fig. 8 Comparison between the acceleration response spectra of the N-S component of the Montenegro earthquake of April 15, 1979, Petrovac record, with the Eurocode 8 design spectrum for firm soil

To obtain the model earthquake, the duration of the strong phase of the actual record has been reduced according to the rules of the complete similitude (time scale factor $S_t = \sqrt{S_L}$ = 2.24), whereas the accelerations remained the same (acceleration scale factor $S_a = 1.0$). Modeled acceleration time history has been integrated and the calculated displacement time history of the model earthquake has been used as the input signal to drive the shaking table. The intensity of the shaking in each subsequent test run has been step-wise increased by adjusting the maximum amplitude of the calculated displacement time history.

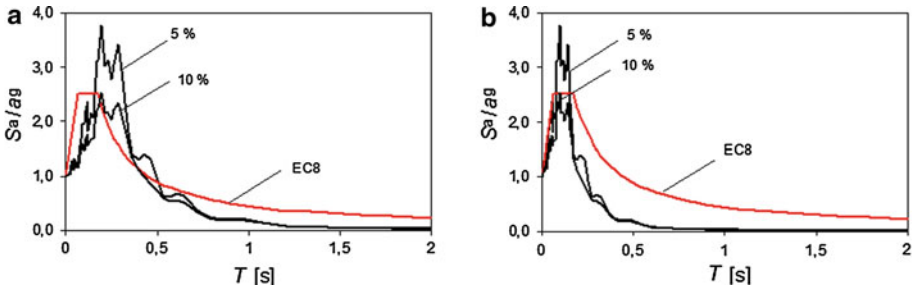

Fig. 9 Correlation between the acceleration response spectra of the model earthquake (**a**) (**b**) model earthquake compressed in time by 2-times with modeled Eurocode 8 design spectrum

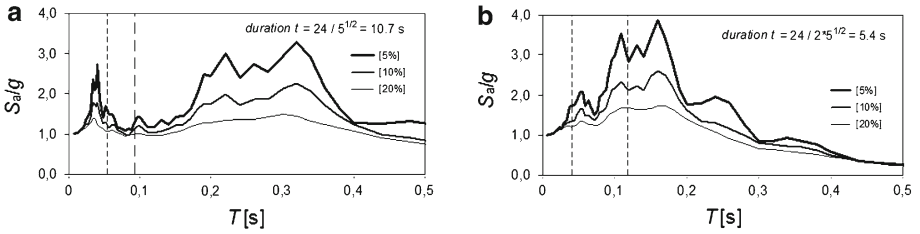

Fig. 10 Absolute acceleration response spectra of the shaking table motion during test runs R100: **a** models M2-1, M2-2, and M1-1 **b** models M1-2, M1-1c, and M1-1d. The range of natural periods of the tested models is indicated with *dashed lines*

In the case of testing of models M2-1, M2-2, and M1-1, mechanical malfunction distorted the shaking-table motion. In order to reduce the error and improve the correlation between the response spectra of the model earthquake and Eurocode 8 design spectrum in the frequency range of maximum amplification (Fig. 9), the duration of the modeled earthquake has been compressed 2-times. Although the malfunction has been repaired, models M1-2, M1-1c, and M1-1d have been subjected to earthquake motion, compressed in time.

Despite a significant shift of peak acceleration values in the acceleration response spectra, both types of simulated earthquakes had similar spectral amplifications in the frequency range of the tested models (Fig. 10). Consequently, both types of simulated earthquakes had similar effects on the tested models.

The models have been tested in a sequence of test runs with intensity adjusted to 5% (R005), 10% (R010), 25% (R025), 50% (R050), 75% (R075) and 100% (R100) of displacement amplitudes, obtained by the integration of the model earthquake. Shaking with intensity of 125% and repeated shaking with intensity of 150% has been needed to cause the collapse of models M2-1 and M1-1d, respectively.

3 Test results and analysis

The failure mechanism did not depend on materials of construction, but depended on structural configuration. Whereas limited stiffness and resistance of the staircase walls in the case of the terraced house models M1 did not prevent the flexural behavior of the walls, orthogonal to seismic excitation, no such phenomena have been observed in the case of the apartment house models M2 with uniformly distributed structural walls in both orthogonal

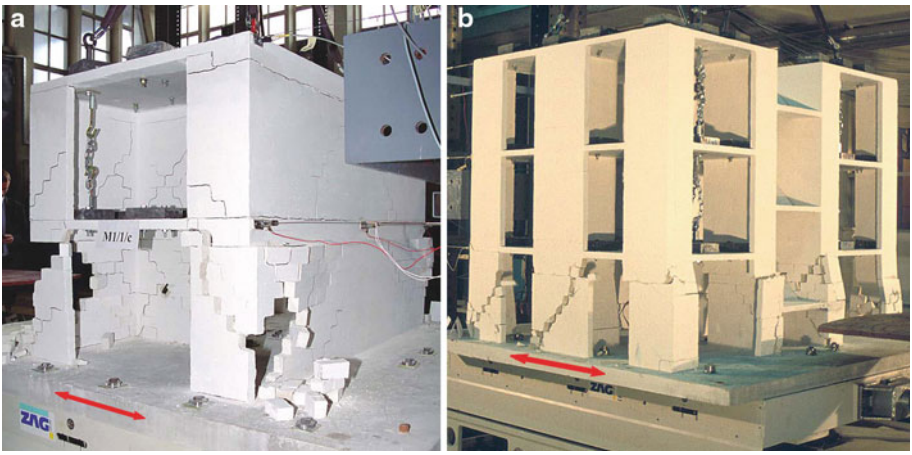

Fig. 11 Confined terraced house model M1-1c (**a**) and (**b**) apartment house model M2-2 at the ultimate state before collapse

directions. In both cases, however, shear cracks, which developed in the walls in the direction of seismic motion, caused severe stiffness degradation, loss of resistance of the structure and final collapse of the models. The unreinforced terraced house model M1-1 and apartment house model M2-1, made of masonry Type 1 exhibited quite brittle behavior and collapsed soon after the occurrence of the first damage, whereas the behavior of similar models M1-2 and M2-2, made of masonry Type 2 was more ductile. Although severely damaged after the attainment of maximum resistance, these models withstood additional shaking before collapse. Typical damage to plain terraced-house and apartment-house model at ultimate state before collapse is shown in Fig. 11. In Fig. 11a, the horizontal flexural cracks in the walls of model M1-1, orthogonal to seismic excitation, can be clearly seen. As a result of partial collapse of the walls on one side of the model at ultimate state, torsional vibration took place, causing diagonally oriented cracks in the walls, orthogonal to seismic excitation.

Vertical confining elements significantly improved the behavior of the terraced house models. Even in the case where the walls have been only partly confined (model M1-1c), the resistance and displacement capacity of the model was improved. In the case where the confining elements have been placed as required by the standard (model M1-1d), the model withstood repeated severe shaking before collapse. The model collapsed when subjected to sinusoidal excitation with frequency which followed the decayed natural frequency of the model.

As can be seen, the damage to structural walls was concentrated in the first story, indicating the prevailing shear type mechanism of seismic behavior. Limited amount of damage to the walls in the upper stories has been observed at collapse in all cases, including confined terraced house models M1-1c and M1-1d. Typical acceleration and displacement response time histories in the initial and non-linear phases of testing of representative models are shown in Figs. 12, 13, 14, and 15. The analysis of vibration response records indicated predominant effect of the first mode of vibration. Typical response shape values, obtained by evaluating, normalizing and averaging several consecutive displacement amplitude peaks of the measured displacement response of the models at individual story levels, are presented in Fig. 16.

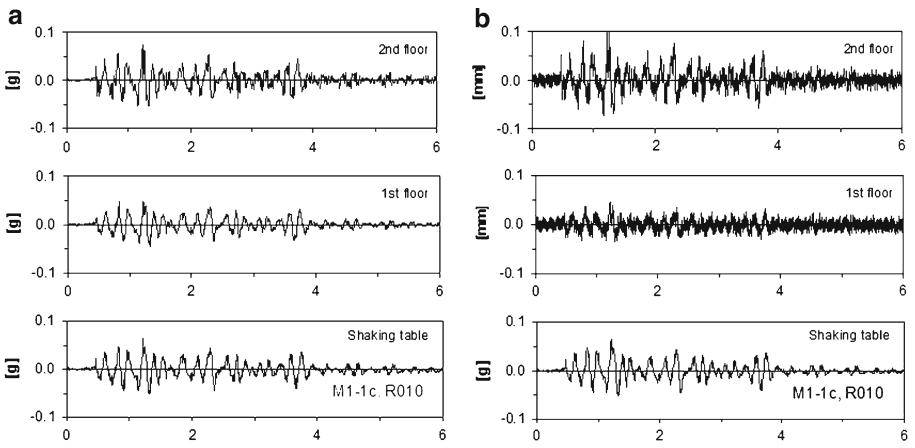

Fig. 12 Typical acceleration (**a**) and (**b**) displacement response of the terrace house model during the initial phase of testing of model M1-1c

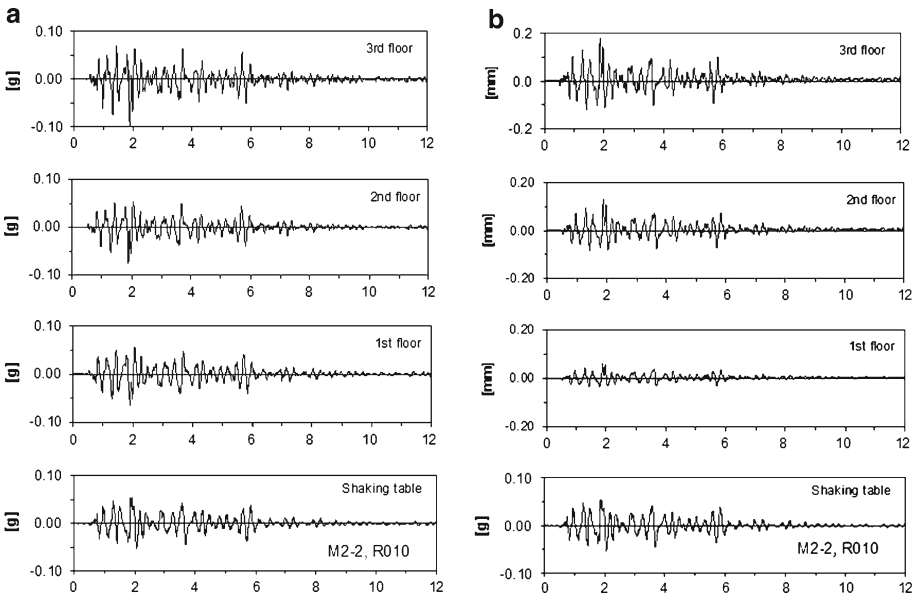

Fig. 13 Typical acceleration (**a**) and (**b**) displacement response of the apartment house model during the initial phase of testing of model M2-2

The first natural frequency of vibration and coefficient of equivalent viscous damping have been evaluated by Fourier analysis of free vibrations, excited by hitting the top floor slab of each model with an impact hammer. The parameters have been measured on virgin models before the beginning of shaking tests as well as after each successive test run. The changes in the first natural frequency of vibration and damping during the shaking table tests can be seen in Table 6.

On the basis of displacement and acceleration response time history records and taking into account the masses of the models, concentrated at each floor level, the relationships between

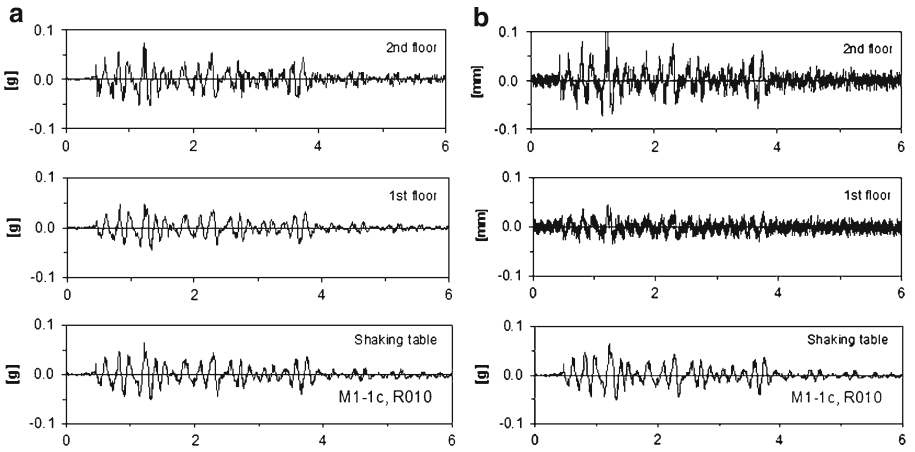

Fig. 14 Typical acceleration (**a**) and (**b**) displacement response of the terrace house model during the non-linear phase of testing of model M1-1c

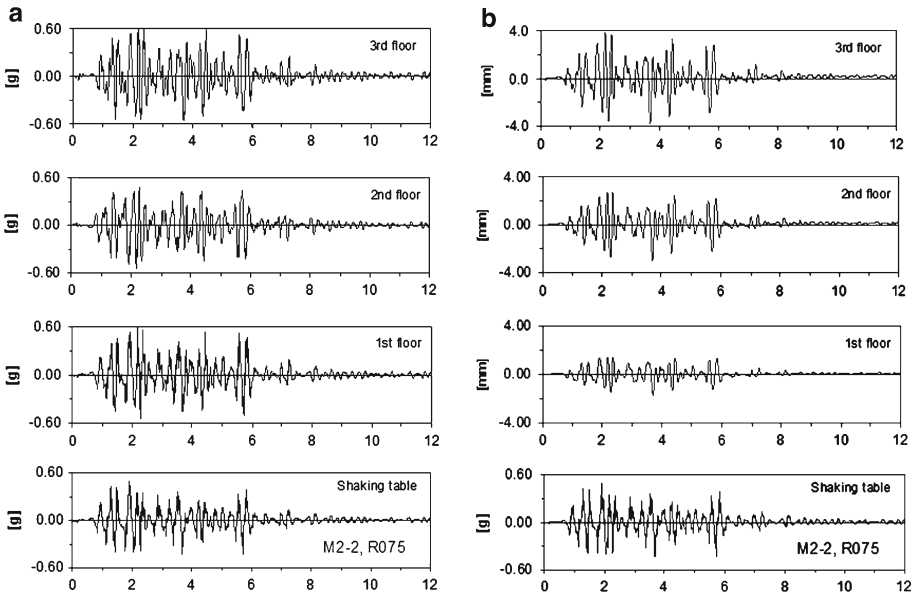

Fig. 15 Typical acceleration (**a**) and (**b**) displacement response of the apartment house model during the non-linear phase of testing of model M2-2

the seismic shear forces developed in the models and displacements have been analyzed. At each instant of time, the seismic shear force has been evaluated as the sum of products of masses, concentrated at the levels of floors m_i (Table 4) and measured acceleration values at the same level a_i, above the story considered: $S_i = \Sigma m_j a_j$ (j = i…n). Typical hysteretic relationships between the story shear and relative story displacements, obtained during the initial and non-linear phases of testing of models M1-1c and M2-2, are presented in Figs. 17 and 18, respectively.

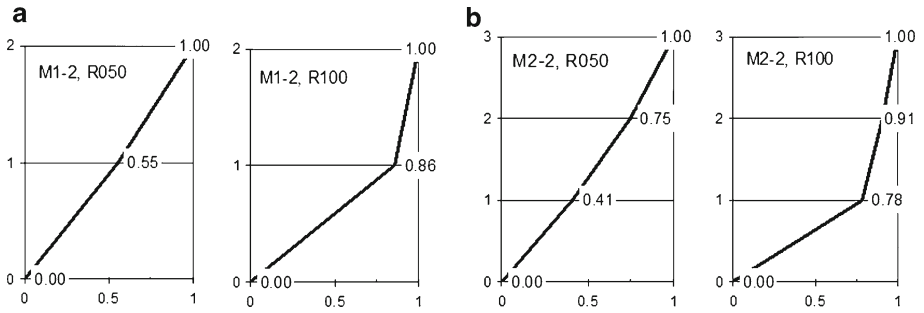

Fig. 16 Typical first vibration mode shapes of (**a**) terraced house building model M1-2 and (**b**) apartment house building model M2-2

Table 6 Changes in first natural frequency of vibration f (Hz) and damping ζ (% of critical) of the tested models during the shaking tests

Model	M1-1		M1-2*		M1-1c*		M1-1d*		M2-1		M2-2	
Test run	f (Hz)	ζ (%)	f (Hz)	ζ (%)	f (Hz)	ζ (%)	f (Hz)	ζ (%)	f (Hz)	ζ (%)	f (Hz)	ζ (%)
Virgin	18.3	6.3	17.0	3.4	23.5	14.7	23.7	7.9	18.8	2.1	12.4	2.0
R005	17.3	4.9	16.1	3.3	21.6	8.9	–	–	–	–	–	–
R010	17.2	5.9	–	–	20.2	9.4	21.1	7.8	18.5	2.9	12.7	2.6
R025	17.1	5.5	13.9	3.3	17.6	8.2	19.2	8.2	18.0	2.2	12.5	2.0
R050	15.0	6.5	9.7	5.3	8.2	7.8	18.0	7.4	17.2	3.2	12.0	2.4
R075	13.8	6.7	8.2	5.8	5.2	16.8	16.2	6.3	16.2	3.2	11.6	2.4
R100	–	–	3.6	9.6	–	–	3.5	11.1	15.1	4.0	10.8	2.9

* Duration of shaking 5.4 s

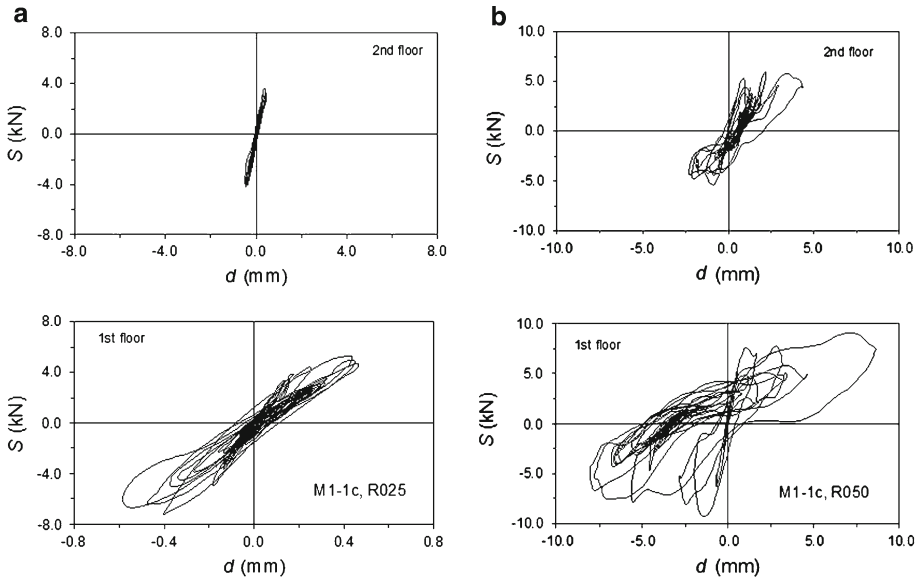

Fig. 17 Typical story shear-relative story displacement hysteresis relationships, obtained by testing of model M1-1c in the linear (**a**) and (**b**) non-linear phase of vibration

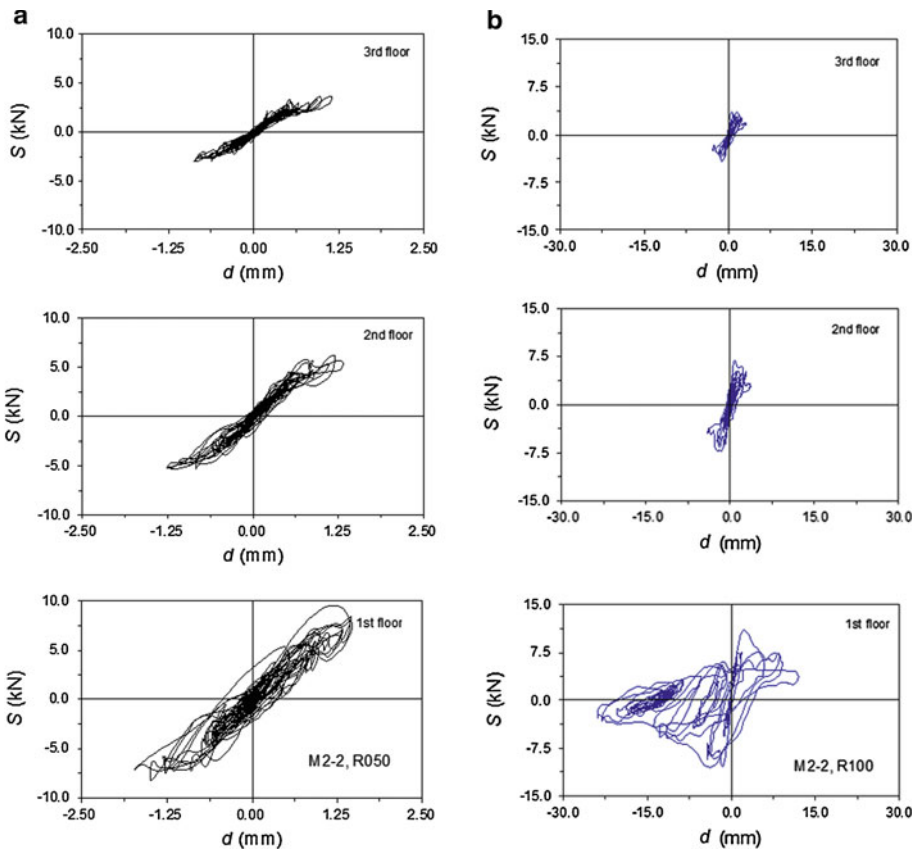

Fig. 18 Typical story shear-relative story displacement hysteresis relationships, obtained during testing of model M2-2 in the linear (**a**) and (**b**) non-linear phase of vibration

On the basis of the observed vibration mode, damage propagation and mechanism of collapse, it can be concluded that story mechanism governed the behavior of the tested models. Consequently, the resistance and displacement capacity of the tested structures can be determined by the resistance curve of the first story of the models. The values of the maximum base shear developed during the individual phases of testing have been calculated as the sum of products of masses, concentrated at the levels of floors m_i and measured maximum values of accelerations at the same level a_i : $BS = \Sigma m_j a_{max,j}$.(j = i…n). The resistance curve of the model under consideration has been evaluated as a relationship between the maximum resisted base shear and corresponding first story drift (relative story displacement), developed in the structure at the same instant of time. Only one point, representing the maximum base shear, has been plotted for each consecutive testing phase. For easier comparison, the base shear and first story relative displacement are expressed in a non-dimensional form of the base shear coefficient, *BSC*, and the first story drift, Φ, respectively. Base shear coefficient is the ratio between the base shear *BS* and the weight of the model above the foundation W : $BSC = BS/W$, whereas the first story drift, Φ, is the ratio between the first story relative displacement, d, and story height, h : $\Phi(\text{in}\%) = (d/h)100$.

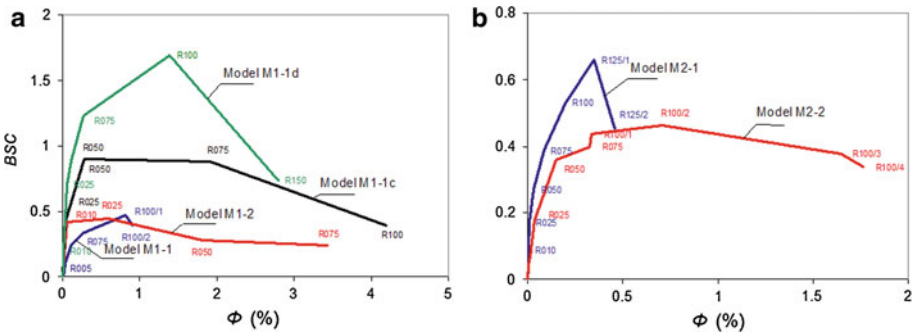

Fig. 19 Seismic resistance curves in the form of the base shear coefficient-first story drift angle relationships for terraced-house models M1 (**a**) and (**b**) apartment house models M2

Following the testing routine, models have been tested by subjecting them to simulated earthquakes with increased intensity of motion in each subsequent test run. However, since the dynamic properties of the models changed as the result of stiffness degradation caused by the damage to structural walls, different structures have been actually tested each time, subjected to a stronger shaking during each subsequent test run (see Table 6). Nevertheless, the curves represent the actual resistance curves of the tested structures reasonably well. The resistance curves are presented separately for the terraced and apartment house models in Fig. 19.

The results of tests are summarized in Table 7, where the values of the actually measured base shear, BS, and first story relative displacement, d, as well as the base shear coefficient, BSC, and story drift, Φ, at the crack (damage) limit, Φ_{cr}, (occurrence of the first significant cracks in the walls), maximum attained resistance, Φ_{Rmax}, and just before collapse, Φ_u, are given for models M1 and M2, respectively. For information, expected prototype BSC values are also given in Table 7. Since the shear mechanism determined the seismic resistance of model buildings, tensile strength of model masonry has been taken into consideration for scaling the model values of BSC. In the case of the models, made of Type 1 masonry, the acceleration scale factor $S_a = S_f/(S_L S_\gamma) = 0.50$ has been taken into account, whereas in the case of the models, made of Type 2 masonry, the acceleration scale factor $S_a = 0.56$ has been considered (see Table 2 for general equation and Table 3 for correlation between the target prototype and actual tensile strength values of model masonry).

The resistance of models built with weaker masonry (masonry Type 2, models M1-2 and M2-2) was smaller than the resistance of equivalent models built with stronger masonry (masonry Type 1, models M1-1 and M2-1). However, the degree of improvement depended also on structural configuration. Increased shear strength of masonry resulted into smaller improvement of lateral resistance in the case of the terraced house models M1 than in the case of the apartment house models M2 with regular structural layout. As can be seen in Table 7, the ratio $BS_{\max,\,M1-1}/BS_{\max,\,M1-2} = 1.39$ has been obtained in the case of the terraced house models M1 and $BS_{\max,\,M2-1}/BS_{\max,\,M2-2} = 1.96$ in the case of the apartment house models M2. If expressed in terms of the base shear coefficient, the differences in resistance are not so large, because they are partly compensated by greater mass of masonry in the case of Type 1 masonry buildings. If referred to prototype buildings, the relationships change because of the actual strength scale factors, which have not been the same for both masonry types.

In the case of both structural types, i.e. terraced house models M1 and apartment house models M2, the behavior of stronger models was brittle (models M1-1 and M2-1 made of

Table 7 Parameters of seismic resistance measured on the models and values referred to prototype buildings at characteristic limit states

Model	Limit state	BS (kN)	d (mm)	BSC_M	BSC_P	Φ (%)
M1-1	Crack limit	3.47	1.35	0.34	0.17	0.26
	Maximum resistance	4.90	4.22	0.47	0.24	0.82
	Before collapse	4.01	4.69	0.39	0.19	0.91
M1-2	Crack limit	3.52	3.09	0.44	0.25	0.60
	Maximum resistance	3.52	3.09	0.44	0.25	0.60
	Before collapse	1.91	17.78	0.24	0.13	3.43
M1-1c	Crack limit	7.21	8.55	0.90	0.45	0.28
	Maximum resistance	7.21	8.55	0.90	0.45	0.28
	Before collapse	4.00	21.77	0.39	0.20	4.20
M1-1d	Crack limit	12.65	1.39	1.23	0.61	0.27
	Maximum resistance	17.47	7.20	1.69	0.85	1.39
	Before collapse	7.57	14.49	0.73	0.37	2.80
M2-1	Crack limit	12.21	1.05	0.53	0.26	0.20
	Maximum resistance	15.19	1.79	0.66	0.33	0.35
	Before collapse	10.43	2.46	0.45	0.23	0.46
M2-2	Crack limit	6.88	1.72	0.40	0.22	0.33
	Maximum resistance	7.74	3.65	0.46	0.26	0.71
	Before collapse	6.17	9.14	0.34	0.19	1.77

Type 1 masonry), whereas the displacement capacity of less resistant models was improved (models M1-2 and M2-2 made of Type 2 masonry). In the specific case tested, this is in good correlation with the results of cyclic lateral resistance tests of model masonry walls. However, additional experimental research is needed to generalize this conclusion.

As regards the displacement capacity of tested structural types, the terraced house models M1-1 and M1-2 withstood larger displacements just before collapse than respective apartment house models M2-1 and M2-2. As can be seen in Table 7, the ratio $\Phi_{u,M1}/\Phi_{u,M2}$ was practically the same in the case of models made of both masonry types. The value of ratio $\Phi_{u,M1-1}/\Phi_{u,M2-1} = 1.98$ has been obtained in the case of Type 1 masonry, whereas in the case of Type 2 masonry, the ratio was $\Phi_{u,M1-2}/\Phi_{u,M2-2} = 1.94$.

The behavior of partly and fully confined models M1-1c and M1-1d has been significantly improved as regards both, lateral resistance and displacement capacity. However, although the confining elements prevented collapse, significant damage occurred in the models' walls at large lateral displacements.

To analyze the differences in energy dissipation capacity, the amount of dissipated hysteretic energy has been compared with input seismic energy in each testing phase (Housner 1959; Bertero and Uang 1992). The cumulative input energy, $E_{inp,cum}$, represented by the work of the actuator from the beginning of test (initial test run $R_1 = R005$) to the end of the test run under consideration (test run R_i), has been evaluated by:

$$E_{inp,cum} = m_e \sum_{R_1}^{R_i} \int_0^{t_0} |a_m(\tau) v_r(\tau)| \, d\tau, \tag{1}$$

Table 8 Cumulative input, E_{inp}, and dissipated hysteretic energy, E_{hys}, at maximum resistance of the models

Model	E_{inp} (Nm)	E_{hys} (Nm)	E_{hys}/E_{inp}
M1-1	–	–	–
M1-2	431	78	0.18
M1-1c	924	342	0.37
M1-1d	1618	667	0.40
M2-1	565	94	0.17
M2-2	1827	630	0.34

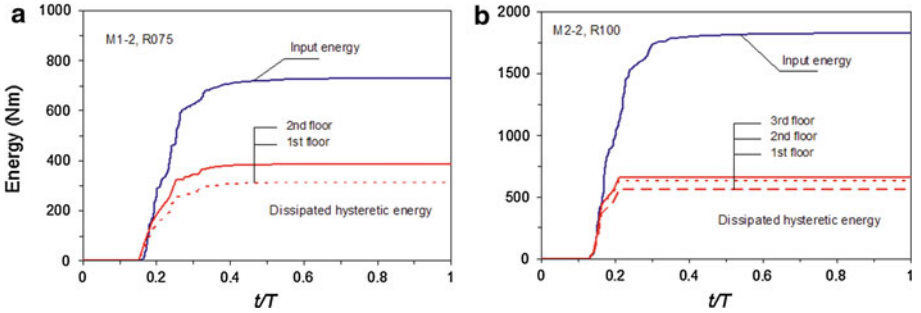

Fig. 20 Hysteretic energy dissipation capacity of apartment house models M2-1 (**a**) and (**b**) M2-2 after the end of test run R100

where $a_m(\tau)$ = the shaking-table acceleration time history at the given instant of time; $v_r(\tau)$ = the relative velocity of the response of the model, idealized as a single degree of freedom system, at the same instant of time; t_0 = the duration of excitation during each individual test run; and m_e = the equivalent mass of the model, idealized as a single degree of freedom system. The actual response of the models has been taken into account by idealizing the tested structure with an equivalent single degree of freedom system (Tomaževič 1987). The equivalent mass, m_e, of the model, idealized as a single degree of freedom system, has been calculated by:

$$m_e = \sum_{i=1}^{n} m_i \Psi_i, \tag{2}$$

where Ψ_i = modal shape vector, and m_i = mass, concentrated at i-th floor level (see Fig. 13 and Table 4 for the first mode of vibration shapes and masses, respectively). The values of $v_r(\tau)$ have been calculated by taking into consideration the measured relative displacement response of the model at the position of the mass of the equivalent single degree of freedom system.

Typical relationships between the calculated cumulative input energy E_{inp} and cumulative dissipated hysteretic energy E_{hys} at the attained maximum resistance of the models are given in Table 8. Although not much can be concluded on the basis of comparison of the absolute values, the ratios between the dissipated and input energy at this particular testing phase confirm the conclusions drawn on the basis of the analysis of the response of models to simulated seismic motion. In the case of the models with improved displacement capacity, the ratio between the dissipated and input energy has been also increased. Typical diagrams, which show the relationship between the input and dissipated energy, however are shown in Fig. 20.

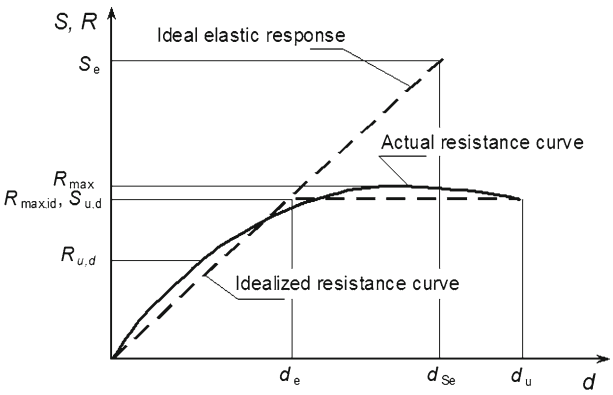

Fig. 21 Definition of structural behavior factor

4 Displacement capacity and structural behaviour factor

4.1 Structural behavior factor

If a regular structure possesses displacement and energy dissipation capacity, it may be designed using conventional elastic analysis model for the ultimate design loads, which are equal to elastic seismic forces, which would develop in an equivalent ideal elastic structure, reduced by a factor, called force reduction factor or structural behavior factor. According to Eurocode 8, "the behavior factor q is an approximation of the ratio of the seismic forces that the structure would experience if its response was completely elastic with 5% viscous damping to the minimum seismic forces that may be used in the design—with a conventional elastic analysis model—still ensuring a satisfactory response of the structure". The definition can be expressed by:

$$q = S_e/S_u, \text{ d}, \tag{3}$$

where S_e = seismic force developed in a completely elastic structure and $S_{u,d}$ = the design seismic load.

The definition is explained in Fig. 21, where the resistance curve of an actual structure, idealized with ideal elastic—ideal plastic relationship, is compared to the response of equivalent ideal elastic one with the same initial stiffness characteristics.

The structure is considered earthquake resistant, if the design resistance, $R_{u,d}$, is equal to or greater than the design seismic load, $S_{u,d}$. Since the elastic analysis methods do not take into consideration the redistribution of seismic loads after yielding of individual structural elements, and the mean values of mechanical properties of materials are reduced by partial safety factors, γ_M, the design resistance of the structure, $R_{u,d}$, is only an approximation of the actual maximum resistance, $R_{max}(R_{max,id})$. In the case that the design resistance of the structure, $R_{u,d}$, is smaller than $R_{max}(R_{max,id})$, the reserve strength (overstrength), expressed in terms of overstrength factor $\rho = R_{max}/R_{u,d}(R_{max,id}/R_{u,d})$, results into increased value of behavior factor:

$$q_\rho = \rho q. \tag{3a}$$

Taking into consideration energy conservation principle and making equal areas below the ideal elastic and idealized elastic-plastic resistance-displacement relationships of the structure

(Fig. 21), the structural behavior factor q can be also expressed in terms of the global ductility factor of the structure under consideration, $\mu_u = d_u/d_e$, where d_e = the displacement of the structure at the idealized elastic limit and d_u = the displacement at ultimate limit, as follows:

$$q = (2\mu_u - 1)^{1/2}. \tag{4}$$

whereas the basic definition (Eq. 3) expresses the behavior factor q in terms of forces, Eq. 4 expresses the definition in terms of global ductility of the structure. Eq. 3 is based on the assumption that maximum displacements of elastic and elastic-perfectly plastic systems with the same initial stiffness are equal, when subjected to the same earthquake. Eq. 4, however, is based on equality of energy potentials of elastic and non-linear systems: the areas under the elastic response line and actual response curve are equal. In other words, Eq. 4 determines also the minimum ductility capacity requirement, which should be fulfilled if the behavior factor q is used for seismic resistance verification:

$$q_{(\text{Eq.3})} \leq q_{(\text{Eq.4})}. \tag{5}$$

This makes possible the use of the idea of reduction of seismic forces also in the case where the resistance curve of the structure, calculated by pushover methods, is used for seismic resistance verification. However, in such a case not only the resistance, but also the displacement capacity of the structure should be verified. In other words, if the seismic resistance of a masonry structure is verified for the design seismic loads, calculated by taking into account the structural behavior factor q, its global ductility should not be less than:

$$\mu_{u,\min} = (q^2 + 1)/2. \tag{6}$$

Basically the same principle is suggested in Eurocode 8 for the determination of the target limit displacement in the case of pushover analysis (Eurocode 2004).

4.2 Displacement capacity and damage limitation

However, if structural behavior factor is determined on the basis of the displacement and ductility capacity of the structure, damage limitation requirement should be taken into account. Taking into consideration fact the values of story drift at characteristic limit states are similar in all cases (see Fig. 16 and Table 7), an attempt has been made to correlate the observed damage, displacement capacity and limit states. On the basis of the results of this and some previous studies (Tomaževič and Weiss 1994; Tomaževič and Klemenc 1997) trends can be seen and ranges of story rotation values at the attainment of characteristic limit states can be evaluated. The following ranges of values of story drift have been obtained (Tomaževič 2007):

- At crack limit: $\Phi_{cr} = 0.2 - 0.4\%$;
- At maximum resistance: $\Phi_{Rmax} = 0.3 - 0.6\%$, and
- At limit state of collapse: $\Phi_u = 2.0 - 4.0\%$.

Similar observations have been reported by other researchers (e.g. Benedetti et al. 1998; Zonta et al. 2001; Alcocer et al. 2004; Naseer 2009). Because of different structural configurations, materials and construction systems, the values at ultimate state near collapse vary substantially. However, in the particular case studied, all models exhibited non-linear behavior with lesser or greater degree of displacement and energy dissipation capacity (see Fig. 19).

In order to analyze the displacement capacity, the experimentally obtained resistance curves have been idealized with bilinear ideal elastic—ideal plastic relationship (Fig. 22). In

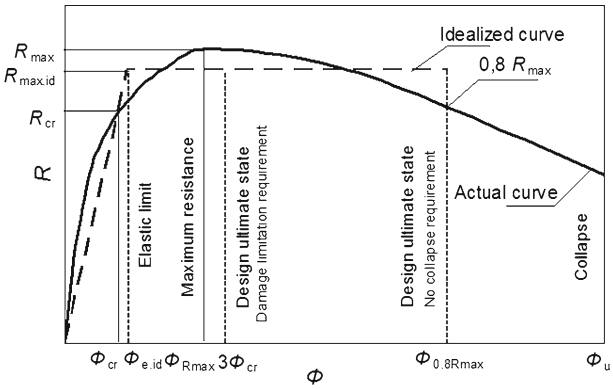

Fig. 22 Idealization of resistance curve and definition of limit states (adapted from Tomaževič 2007)

the idealization of the experimental curve, the initial slope of the idealized envelope (effective stiffness, K_e) is defined with a secant stiffness, obtained by connecting a conventionally defined point on the segment of the experimental curve between the test runs, where the first damage and significant change of the first story stiffness has occurred, with the origin. The principle of best fitting of the idealized bi-linear relationship with the experimental curve has been followed. The ultimate resistance of the idealized envelope $R_{max,id}$ is calculated by taking into account the equal energy dissipation capacities of an actual and idealized structure: the areas below the actual and idealized curves should be equal. Knowing the effective stiffness and idealized maximum resistance, story drift at the idealized elastic limit, $\Phi_{e,id}$, can be calculated. As a result of such idealization, story drift at the idealized elastic limit, $\Phi_{e,id}$, is usually greater than story drift at the occurrence of cracks, Φ_{cr}.

In the idealization of the experimentally obtained resistance envelope, story drift at the point where the resistance of the structure degrades to 80% of the maximum, is usually defined as the ultimate. In other words, story drift at 20% of strength degradation is considered as the maximum value which can be taken into consideration for the evaluation of the idealized design ultimate global ductility factor of the structure: $\mu_{u,d} = \Phi_{0,8Rmax}/\Phi_{e,id}$. It is assumed that a ductile structure, although severely damaged, will resist such a displacement without risking collapse (no collapse requirement).

Four main limit states, which are used in seismic resistance verification and determine the usability of buildings, are defined on the resistance curve:

- Crack (damage) limit state, where the first cracks occur in the walls, causing evident changes in stiffness of the structural system (R_{cr}, Φ_{cr}). Crack limit on the resistance curve is sometimes associated with the serviceability limit state of the structure;
- Maximum resistance (R_{max}, Φ_{Rmax});
- Design ultimate limit state, where the resistance of the system degrades below the acceptable level ($0,8R_{max}$, $\Phi_{0,8Rmax}$). Conventionally, 20% of degradation of maximum resistance is acceptable. Consequently, part of the resistance curve, where the resistance degrades below 80% of the maximum, is no more considered for design purposes. It only provides information about additional ductility and energy dissipation capacity, i.e. additional safety of the structure;
- Limit of collapse, defined by partial or total collapse of the structure (R_u, Φ_u).

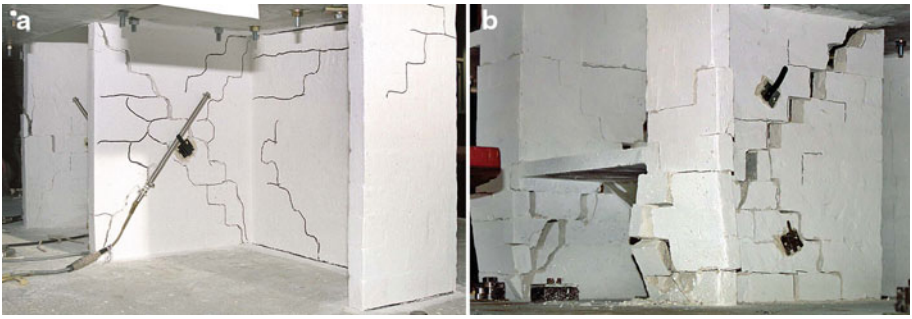

Fig. 23 **a** Damage grade 3, observed after the attainment of maximum resistance (Model M1-1c, R050, $\Phi_{d,u} = 0.9\%$) and **b** damage grade 4–5, observed just before collapse (Model M2-2, R100/3, $\Phi_u = 1.77\%$)

A recent study indicated (Tomaževič 2007) that in the case where the shear behavior prevails, characteristic damage grades as defined by EMS-98 scale (European 1998) can be attributed to so defined characteristic limit states as follows:

- Grade 2 ("slight structural damage, cracks in many walls" by EMS-98): formation of the first, hardly visible diagonally oriented cracks in the middle part of the wall. Light damage can be attributed to crack (damage) limit.
- Grade 3 ("moderate structural damage, cracks in many walls" by EMS-98): increased number of cracks with limited width (less than 0,2 mm wide), oriented diagonally in both diagonal directions. This is moderate, repairable damage, which may be defined as acceptable damage at serviceability limit state, develops somewhat after the attainment of maximum resistance.
- Grade 4 ("heavy structural damage, serious failure of walls" by EMS-98): increased number of more than 1 mm but less than 10 mm wide diagonally oriented cracks. Crushing of individual masonry units. This is heavy damage, which is in most cases repairable, but sometimes repair is not economical. Grade 4 damage is observed near the point which is defined as the design ultimate limit state, where the actual resistance of the structure degrades to 80% of the maximum.
- Grade 5 ("total or near total collapse" by EMS-98): increased width (more than 10 mm) of cracks, crushing of units along both wall diagonals. Severe strength degradation and final collapse. It is obvious that grade 5 damage defines the ultimate state of collapse.

Taking into consideration the acceptable level of damage, the deformations, where the masonry buildings are safe and usable, attain the deformations at maximum resistance and slightly beyond. In this range, damage to structure, not exceeding grade 3 damage, is expected. The range of deformations, where the masonry building is still safe but no longer usable (no collapse requirement), spans from the maximum resistance to the ultimate limit state. In this range of deformations, damage grade 3 to damage grade 4 is expected. Typical damage observed at these states is shown in Fig. 23.

As the analysis of the observed behavior of tested models indicated, damage grade 3 develops slightly after the attained maximum resistance. The analysis further indicated that such damage generally occurs at story drifts, equal to approximately 3-times of story drift at the occurrence of the first cracks in the walls, or 3-times of story drift at the idealized elastic limit. Since damage grade 4 is usually not economical to repair, not only the resistance degradation (80% of the maximum resistance is considered as design ultimate), but also the damage limitation requirement has been considered when evaluating the behavior factor q in this study.

If the occurrence of damage grade 3 is considered as appropriate measure for damage limitation, displacement capacity of a masonry structure beyond the relative story displacement (drift), equal to 3 times of displacement (drift) at the occurrence of the first cracks in structural walls, is not taken into account in earthquake resistance verification. Considering the idealized curve, the design ultimate state may be defined by either the displacement (drift) value where the resistance degrades to 80% of the maximum, or the displacement (drift) value, which attains 3-times the value of the displacement (drift) at the idealized elastic limit, whichever is less:

$$\Phi_{\mathrm{d,u}} = \min\{\Phi_{0,8\mathrm{Rmax}}; 3\Phi_{\mathrm{cr}}\}. \tag{7}$$

It is obvious that resistance degradation represents the no collapse requirement, whereas the damage limitation requirement is represented by the limited story drift. If the smaller value is considered for the evaluation of design parameters, such as behavior factor q, both requirements will be fulfilled at the same time. It is therefore, not needed that the masonry buildings be checked for the serviceability limit state. As has been observed within the framework of this study, the limiting value of story rotation $\Phi_{\mathrm{d,u}} = 3\Phi_{\mathrm{cr}}$ $\left(3\Phi_{\mathrm{e,id}}\right)$ prevailed in most cases.

4.3 Evaluation of structural behavior factor q

The following ranges of values of structural behavior factor q are proposed in Eurocode 8 for different masonry construction systems:

- for unreinforced masonry: $q = 1.5 - 2.5$,
- for confined masonry: $q = 2.0 - 3.0$,
- for reinforced masonry: $q = 2.5 - 3.0$.

Although the use of values at the lower limits of proposal is recommended, the National Annexes may specify the values to be used in individual EU member states. Using advantage of the experimental data, an attempt has been made to verify the proposed code values for unreinforced and confined masonry.

Taking into consideration the basic, simple definition of behavior factor q, given by Eq. 3, the value of factor q is evaluated as a ratio between the response of an ideal elastic structure and the response of an actual non-linear structure to the same strong earthquake. In the particular case studied, the maximum seismic force developed in the elastic system, subjected to shaking-table motion where the analyzed model attained its maximum resistance, has been compared to maximum (idealized) resistance of the same model, obtained by testing.

EAVEK, a commercial computer program for seismic analysis of multi-story buildings, has been used for the calculation of the seismic response of the elastic structures (Fajfar and Kilar 1992). In the calculation, the models have been modeled as simple multi-degree of freedom shear systems. Story stiffnesses, evaluated on the basis of the measured story shear-story drift relationships (Figs. 17a and 18a), obtained in the initial phases of testing, and masses, concentrated at floor levels (Table 4), have been used as input parameters. The maximum values of the base shear and first story drift of the calculated ideal elastic response are summarized in Table 9. The calculated values are given in the non-dimensional form of the base shear coefficient, BCS_{e}, and first story drift, Φ_{e}. It is interesting to see that the calculated maximum values of the elastic drift, Φ_{e}, are in most cases close to the experimentally observed values of the story drift at the crack limit, Φ_{cr}. In the same table, the resulting values of behavior factor q obtained by the basic simple definition (Eq. 3), are also given.

Typical examples of evaluation of factor q are shown in Figs. 24, 25 and 26 for the terraced, confined terraced and apartment house models, respectively.

Table 9 Values of structural behavior factor $q_{(\mathrm{Eq.3})}$, evaluated as a ratio between the calculated elastic response (BSC_e) to excitation in the test run where the maximum resistance has been attained, and the actual maximum resistance (BSC_max)

Model	BSC_e	Φ_e (in %)	BSC_max	Φ_cr (in %)	$q_{(\mathrm{Eq.3})} = BSC_\mathrm{e}/BSC_\mathrm{max}$
M1-1	0.74	0.43	0.47	0.26	1.56
M1-2	0.91	0.11	0.44	0.60	2.05
M1-1c	2.19	0.43	0.90	0.28	2.43
M1-1d	2.80	0.33	1.69	0.27	1.65
M2-1	1.05	0.13	0.66	0.20	1.59
M2-2	0.83	0.31	0.46	0.33	1.78

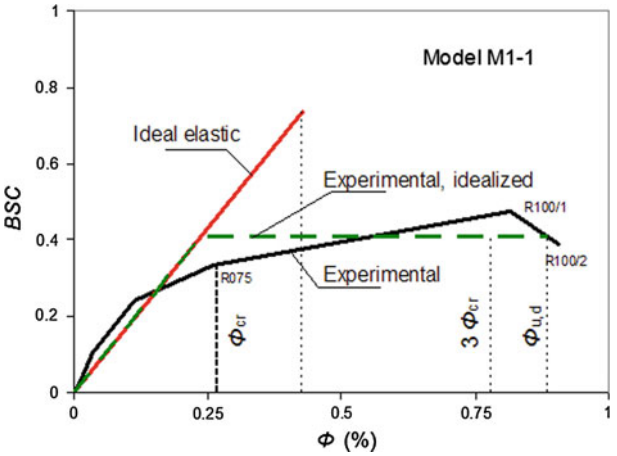

Fig. 24 Evaluation of factor q for the terraced house model M1-1

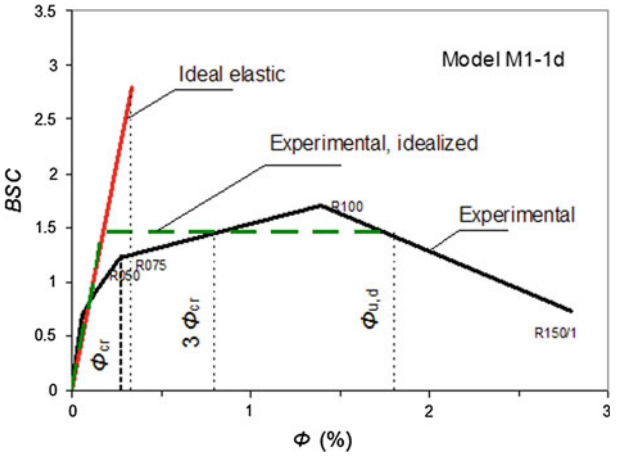

Fig. 25 Evaluation of factor q for the confined terraced house model M1-1d

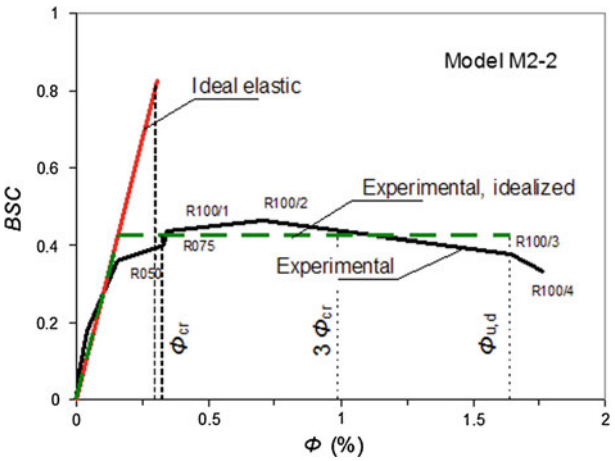

Fig. 26 Evaluation of factor q for the apartment house model M2-2

Table 10 Values of structural behavior factor $q_{(\mathrm{Eq.4})}$, evaluated on the basis of available ductility ($\mu_\mathrm{u} = \Phi_{0.8\mathrm{Rmax}}/\Phi_{\mathrm{e,id}}$) and damage limitation requirements ($\mu_\mathrm{u} = 3\Phi_\mathrm{cr}/\Phi_{\mathrm{e,id}}$)

Model	$\Phi_{\mathrm{ei,d}}$ (in %)	$\Phi_{0.8\mathrm{Rmax}}$ (in %)	Φ_cr (in %)	$3\Phi_\mathrm{cr}$ (in%)	$q_{(\mathrm{Eq.4})} = (2\mu_u - 1)^{1/2}$			
					$\mu_\mathrm{u} = \Phi_0.8\mathrm{Rmax}/\Phi_{\mathrm{ei,d}}$		$\mu_\mathrm{u} = 3\Phi_\mathrm{cr}/\Phi_{\mathrm{ei,d}}$	
					μ_u	q	μ_u	q
M1-1	0.24	0.89	0.26	0.78	3.70	2.53	3.25	2.35
M1-2	0.05	1.20	0.60	0.16	24.00	6.85	3.20	2.32
M1-1c	0.17	2.60	0.28	0.84	15.29	5.44	4.94	2.98
M1-1d	0.17	1.81	0.27	0.81	10.65	4.50	4.76	2.92
M2-1	0.07	0.42	0.20	0.60	6.00	3.32	8.57	4.02
M2-2	0.16	1.65	0.33	0.99	10.31	4.43	6.18	3.37

The values of behavior factor q, evaluated on the basis of the global ductility of the tested models (Eq. 4), are given in Table 10. As a result of definition of initial story stiffness for the calculation of elastic response, the story drift at idealized elastic limit, $\Phi_{\mathrm{e,id}}$, is smaller than the story drift at the first cracking of the walls, Φ_cr. Consequently, the ductility values are relatively high. In the analysis, the actual displacement capacity, i.e. ductility factor evaluated by considering the no collapse requirement $\Phi_{\mathrm{d,u}} = \Phi_{0.8\mathrm{Rmax}}$, as well as displacement capacity, limited in order to prevent excessive damage to structural walls, i.e. ductility factor evaluated by considering the damage limitation requirement $\Phi_{\mathrm{d,u}} = 3\Phi_\mathrm{cr}$, have been considered. As can be seen, the values of factor q in Table 10 are greater than the values given in Table 9 in all cases.

The comparison of values given in Table 10 also indicates, that in the case where the actual displacement capacity is taken into consideration, the differences observed in the behavior of unreinforced masonry models reflect in the values of behavior factor q (like brittle behavior of models M1-1 and M2-1 against improved behavior of models M1-2 and M2-2—see Fig. 16). In the case of the terraced house models with confined structural walls (models M1-1c and M1-1d), the values are higher than in the case of the respective plain

masonry structures. However, if the values of behavior factor are evaluated by taking into consideration damage limitation requirement, the differences in factor q, evaluated for different structural types, are not significant. Moreover, the values, evaluated on the basis of experimental results, are well within the range of values, proposed by the code for seismic resistance verification of unreinforced and confined masonry structures. Although significant differences in the behavior have been observed with regard to different masonry materials and construction systems, damage limitation requirements limit the use of the available displacement and energy dissipation capacity in the design. Although all tested types of structures will fulfill the safety requirements of the code, their actual safety level will not be the same.

4.4 Design resistance capacity and overstrength

It has to be pointed out, that the values of behavior factors q, given in Tables 9 and 10, have been evaluated by taking into consideration the actual, and not the design resistance capacity of the tested models. Therefore, these values represent a safe level of seismic force reduction also in the case where a pushover method is used for seismic resistance verification.

As has been mentioned, conventional elastic analysis methods do not consider redistribution of seismic forces. Also, mechanical characteristics of materials are reduced with partial safety factors so that, consequently, the design resistance of the structure is to a greater or lesser extent smaller than the actual one. According to definition, the values of behavior factor q may be modified by considering the possible overstrength resulting from the use of specific design methodology (Eq. 3a). On the basis of analysis of more than 40 unreinforced masonry buildings, Magenes (2006) reported mean values of overstrength factor, ρ, ranging from 1.8 to 2.4, depending on construction system.

To estimate the overstrength resulting from the reduction of mechanical characteristics of masonry as required by Eurocode 8, the resistance of the tested models has been evaluated with a pushover method (Tomaževič and Weiss 1990), where the resistance curve of the critical story, which determines the relationship between the resistance and story drift, is obtained as a superposition of idealized resistance curves of all walls in the critical story. To calculate the design resistance of the tested models, instead of the mean values of the tensile strength of masonry, given in Table 3, characteristic values have been taken into account. Two different values of partial safety factor for masonry, γ_{M}, have been taken into consideration, namely $\gamma_M = 1.5$, representing design situation in the case of good quality control, and $\gamma_M = 2.0$, representing the average design and construction situation.

The results of calculations are given in Table 11. In the table, the calculated maximum values of the base shear coefficient, $BSC_{\mathrm{d,max}}$, are correlated with the experimental ones, BSC_{max}. Unexpectedly great differences between the experimental and calculated values of seismic resistance in the case of the partly and fully confined terraced-house models (Models M1-1c and M1-1d) are the consequence of requirements of Eurocode, which do not allow that the confining elements (tie-columns) be taken into account as lateral load resisting elements of the structure. The resulting values of overstrength factors, ρ, are also given in Table 11. As can be seen, substantial overstrength has been be observed, although a mechanism model has been used for the calculation of design resistance of the tested model structures. Similar values of overstrength factors have been reported by Magenes (2006).

Table 11 Comparison between the maximum experimental and calculated (design) resistance of tested models

Model	Experimental BSC_{max}	Calculated $BSC_{d,max}$		Overstrength $BSC_{max}/BSC_{d,max}$	
		$\gamma_M = 1.5$	$\gamma_M = 2.0$	$\gamma_M = 1.5$	$\gamma_M = 2.0$
M1-1	0.47	0.32	0.32	1.48	1.49
M1-2	0.44	0.35	0.31	1.28	1.42
M1-1c*	0.90	0.32	0.32	2.80	2.83
M1-1d*	1.69	0.32	0.32	5.27	5.32
M2-1	0.66	0.42	0.40	1.57	1.64
M2-2	0.46	0.33	0.29	1.42	1.61

* According to Eurocode, vertical confining elements should not be considered as lateral load resisting elements of confined masonry structures

5 Conclusions

The results of shaking table tests of a series of 1:5 scale masonry building models have been used for the evaluation of values of structural behavior factor q, seismic force reduction factor proposed by Eurocode 8 for the calculation of design seismic loads for masonry structures. Six models have been tested, representing prototype buildings of two different structural configurations and built with two different types of masonry materials.

The experimental study indicated that, in addition to construction system (plain, confined masonry) and mechanical characteristics of masonry materials, seismic behavior and displacement capacity of masonry buildings depend also on structural configuration. Consequently, although such tests are helpful, the values of behavior factor q cannot be assessed by means of only ductility tests of individual structural walls. In order to assess realistic values of reduction factors, experimental testing should be carried out. Numerical simulation based on the input data obtained by testing of individual walls is not enough.

As indicated by this study, all tested types of masonry buildings exhibited displacement capacity, which allows the reduction of elastic seismic forces in the case where conventional elastic analysis methods are used for seismic resistance verification. It has been also shown that besides displacement and energy dissipation capacity, damage limitation requirements should be taken into account when evaluating the values of behavior factors. To limit the damage caused by the design earthquake, only part of the available displacement and ductility capacity of the structure should be taken into consideration for the assessment of values of structural behavior factor q.

The analysis of experimental results has shown, that the values at the upper limit of the Eurocode 8 proposed range of values of structural behavior factor q for unreinforced and confined masonry construction systems, i.e. $q = 2.5$ in the case of the regular unreinforced, and $q = 3.0$ in the case of the regular confined masonry structures are adequate, if pushover methods are used for seismic resistance verification. However, in this case, the calculated displacement capacity of the structure should be verified and compared with displacement demand.

In the case where elastic analysis methods are used and significant overstrength is expected, the proposed values are conservative. However, additional research and parametric studies are needed to propose the modifications.

Acknowledgments The research discussed in this article has been part of the research program, financed by the Ministry of High Education, Science and Technology of the Republic of Slovenia under grant No. P2-0274. A significant part of it has been co-financed by the Deutsche Gesellschaft für Mauerwerksbau, contract No. 1527/99, within the framework of a research project, jointly carried out by the Civil Engineering Faculty of the University of Dortmund, Institut für Bauforschung Aachen and Slovenian National Building and Civil Engineering Institute. Prototype walls and masonry units have been tested in Germany, whereas the shaking-table tests of models of buildings have been carried out in Slovenia. The authors would like to acknowledge the contribution of their former colleague Dr V. Bosiljkov to the success of the experimental phase of the project.

References

Alcocer SM, Arias JG, Flores LE (2004) Some developments on performance based seismic design of masonry structures. In: Fajfar P, Krawinkler H (eds) Performance-based seismic design. Concepts and implementation. PEER Report 2004/05. Berkeley, pp 33–44

Benedetti D, Carydis P, Pezzoli P (1998) Shaking table tests on 24 simple masonry buildings. Earthq Eng Struct Dyn 27:67–122

Bertero V, Uang CM (1992) Issues and future directions in the use of an energy approach for seismic resistant design of structures. In: Fajfar P, Krawinkler H (eds) Nonlinear seismic analysis and design of reinforced concrete buildings. Elsevier, London, pp 3–22

Da Porto F, Grendene M, Modena C (2009) Estimation of load reduction factors for clay masonry walls. Earthquake engineering and structural dynamics, doi:10.1002/eqe.887

Eurocode 8 (2004) Design of structures for earthquake resistance, Part 1: general rules, seismic actions and rules for buildings. EN 1998-1:2004. CEN, Brussels

European Macroseismic Scale 1998 (1998) Grünthal G (ed) European Seismological Commission, Luxemburg

Fajfar P, Kilar V (1992). EAVEK: supplement to version 3.0. Faculty of Civil Engineering and Geodesy, IKPIR: Ljubljana (in Slovene)

Harris GH, Sabnis GM (1999) Structural modeling and experimental techniques. CRC Press, Boca Raton

Housner GW (1959) Behavior of structures during earthquakes. J Struct Division ASCE 85(4):109–129

Langhaar HL (1951) Dimensional analysis and theory of models. Wiley, New York

Magenes, G (2006) Masonry building design in seismic areas: recent experiences and prospects from a European point of view. In: The first European conference on earthquake engineering and seismology. CD-ROM, Geneva, Keynote Address K9: paper 4009

Moroni MO, Astroza M, Gomez J (1992) Seismic force reduction factors for masonry buildings. In: Proceedings 10th world conference on earthquake engineering, vol.8. Balkema, Rotterdam, pp 4521–4524

Naseer A (2009) Performance behavior of confined brick masonry buildings under seismic demand. Doctoral dissertation, NWFP University of Engineering and Technology, Peshawar

Oetes A, Loering S (2006) On the behavior of masonry buildings subjected to seismic loads. Bautechnik, 83(2): 125–138 (in German)

Tomaževič M (1987) Dynamic modelling of masonry buildings: story mechanism model as a simple alternative. Earthq Struct Dyn 15(6):731–749

Tomaževič M, Weiss P (1990) A rational, experimentally based method for the verification of earthquake resistance of masonry buildings. In: Proceedings fourth U.S. national conference on earthquake engineering, vol. 2. Earthquake Engineering Research Institute, El Cerrito, pp 349–358

Tomaževič M, Velechovsky T (1922) Some aspects of testing small-scale masonry building models on simple earthquake simulators. Earthq Eng Struct Dyn 21(11):945–963

Tomaževič M, Weiss P (1994) Seismic behavior of plain and reinforced-masonry buildings. J Struct Eng ASCE 120(2):323–338

Tomaževič M, Klemenc I (1997) Verification of seismic resistance of confined masonry buildings. Earthq Eng Struct Dyn 26(10):1073–1088

Tomaževič M (2007) Damage as a measure for earthquake-resistant design of masonry structures: Slovenian experience. Can J Civil Eng 34(11):1403–1412

Zonta D, Zanardo G, Modena C (2001) Experimental evaluation of the ductility of a reduced-scale reinforced masonry building. Mater Struct 34:636–644